OXFORD

Cerebral Cortex, 2022, **32**, 5555–5568
https://doi.org/10.1093/cercor/bhac035
Advance access publication date 12 February 2022
Original Article

Characterization of resting functional MRI activity alterations across epileptic foci and networks

Lucas E. Sainburg[1,2], Aubrey A. Little[3], Graham W. Johnson[1,2], Andrew P. Janson[2], Kaela K. Levine[2], Hernán F.J. González[1,2], Baxter P. Rogers[1,2], Catie Chang[1,2,4], Dario J. Englot[1,2,4,5], Victoria L. Morgan[1,2,5,*]

[1]Department of Biomedical Engineering, Vanderbilt University, Nashville, TN 37212, USA,
[2]Department of Radiology and Radiological Sciences, Institute of Imaging Science, Vanderbilt University Medical Center, Nashville, TN 37212, USA,
[3]Department of Biomedical Engineering, Yale University, New Haven, CT 06520, USA,
[4]Department of Electrical and Computer Engineering, Vanderbilt University, Nashville, TN 37212, USA,
[5]Department of Neurological Surgery, Vanderbilt University Medical Center, Nashville, TN 37212, USA

*Corresponding author: Department of Radiology and Radiological Sciences, Institute of Imaging Science, Vanderbilt University Medical Center, R0102 Medical Center North, 1161 21st Ave South, Nashville, TN 37232, USA. Email: victoria.morgan@vanderbilt.edu

Brain network alterations have been studied extensively in patients with mesial temporal lobe epilepsy (mTLE) and other focal epilepsies using resting-state functional magnetic resonance imaging (fMRI). However, little has been done to characterize the basic fMRI signal alterations caused by focal epilepsy. Here, we characterize how mTLE affects the fMRI signal in epileptic foci and networks. Resting-state fMRI and diffusion MRI were collected from 47 unilateral mTLE patients and 96 healthy controls. FMRI activity, quantified by amplitude of low-frequency fluctuations, was increased in the epileptic focus and connected regions in mTLE. Evidence for spread of this epileptic fMRI activity was found through linear relationships of regional activity across subjects, the association of these relationships with functional connectivity, and increased activity along white matter tracts. These fMRI activity increases were found to be dependent on the epileptic focus, where the activity was related to disease severity, suggesting the focus to be the origin of these pathological alterations. Furthermore, we found fMRI activity decreases in the default mode network of right mTLE patients with different properties than the activity increases found in the epileptic focus. This work provides insights into basic fMRI signal alterations and their potential spread across networks in focal epilepsy.

Key words: mesial temporal lobe epilepsy; fMRI; ALFF.

Introduction

The view of mesial temporal lobe epilepsy (mTLE) and other focal epilepsies as brain network disorders is now well established (Davis et al. 2021). Brain network alterations in mTLE have been studied extensively using functional connectivity (FC) measured from resting-state functional magnetic resonance imaging (fMRI) (Bettus et al. 2009, 2010; Morgan et al. 2010; Pereira et al. 2010; Pittau et al. 2012; Englot et al. 2017). However, fMRI measures blood oxygenation, which is only an indirect reflection of neural activity, and little is known about the fundamental changes in the fMRI signal caused by mTLE and other focal epilepsies.

A basic measure of spontaneous activity in the resting-state fMRI signal, the amplitude of low-frequency fluctuations (ALFF) (Zang et al. 2007), has been shown to be increased in mesial temporal structures (Zhang et al. 2010, 2015) and decreased in regions of the default mode network (DMN) (Zhang et al. 2010, 2015; Wei et al. 2016) in mTLE. Furthermore, Zhang et al. showed that subcortical and cortical regions that show frequent interictal spike activity in mTLE also demonstrate ALFF increases (Zhang et al. 2010). These studies indicate that there are consistent abnormalities in the fMRI signal in mTLE involving the epileptic focus which may be linked to interictal activity. In this work, we will use the terms "fMRI activity" and "ALFF" synonymously to refer to these signal changes, with ALFF as the quantification of fMRI activity.

The goal of this work was to use mTLE as the model to characterize how focal epilepsy affects the resting-state fMRI signal in the epileptic focus and the potential spread of these alterations across epileptic networks. In this work, our use of the term "spread" refers to the idea that the most significant and primary change in the activity across the group occurs in the epileptic focus but can also be detected in other regions of the network in individual patients in a less uniform manner. Toward this goal, we quantified fMRI activity alterations by assessing ALFF differences between mTLE patients and controls. Next, we evaluated evidence of potential epileptic fMRI activity spread across the network using four complementary methods. First, networks of regional fMRI activity covariance across subjects were constructed similar to

Received: October 28, 2021. **Revised:** January 19, 2022. **Accepted:** January 24, 2022

previously studied structural covariance networks (He et al. 2007). This was followed by associating this regional fMRI activity covariance to FC. Next, by incorporating diffusion MRI, we quantified the fMRI activity along white matter tracts connecting regions of the network, given the growing evidence that fMRI activations in white matter are modulated during tasks and are related to regional glucose metabolism (Ding et al. 2018; Mishra et al. 2020; Guo et al. 2022). Lastly, we evaluated potential spread of epileptic fMRI activity by assessing the linear interdependence of the fMRI activity changes between the epileptic focus and other regions. We then investigated the associations of these fMRI activity changes with the severity and progression of mTLE to determine their clinical relevance. Finally, to further understand the properties and origins of these alterations, we probed their frequency specificity, which has been shown to be relevant in other epilepsy disorders (Wang et al. 2014; Gupta et al. 2017; Tan et al. 2018). Overall, we hypothesized that epileptic fMRI activity alterations in mTLE spread from the epileptic focus to other regions, become more pronounced with severity and progression of epilepsy, and are associated with specific frequencies in the fMRI signal. If evidence for this hypothesis is found in this cohort, it would support the potential of fMRI to help localize the seizure focus and to quantify the evolution of this disease.

Materials and methods

Subjects

Drug-refractory unilateral mTLE patients ($n = 47$) were recruited for this study after a series of testing to localize the seizure focus, including structural magnetic resonance imaging (MRI), scalp electroencephalography (EEG), seizure semiology, and positron emission tomography (PET), with a few patients also undergoing stereo-EEG (SEEG). Inclusion criteria for patients were either signs of mesial temporal sclerosis (MTS) on MRI or postoperative pathology, mesial temporal gliosis on postoperative pathology, or concordant localization of the focus with both EEG and PET. Patients with other significant structural abnormalities or who had signs of bilateral mTLE were excluded. In addition, 96 healthy controls were enrolled. The Vanderbilt University Institutional Review Board approved the use of human subjects for this study and written consent was acquired from all subjects prior to participation.

Imaging

All imaging was performed on a Philips 3T MRI scanner (Best, Netherlands) using a 32-channel head coil. Each subject underwent a T1-weighted 3D scan for segmentation (1 mm isotropic), a T1-weighted 2D scan in the same slice orientation as the functional images for spatial normalization and segmentation (1 × 1 × 3.5 mm with a 0.5-mm gap), 2 consecutive 10-min T2*-weighted eyes-closed resting-state fMRI scans (3 × 3 × 3.5 mm with a 0.5-mm gap, repetition time = 2 s, echo time = 35 ms), and a diffusion-weighted imaging (DWI) scan for tractography (50 slices, 2.5 mm isotropic, one $b = 0$ volume acquisition, and a single-shell of $b = 1{,}600$ s/mm^2 with 92 directions). A pulse oximeter and respiratory belt collected cardiac and respiratory fluctuations for fMRI preprocessing. Imaging data were acquired before and after a scanner software upgrade that required data harmonization, as described in following sections.

Segmentation

The T1-weighted 3D images were segmented into white matter, gray matter, and cerebrospinal fluid masks using SPM12 (https://www.fil.ion.ucl.ac.uk/spm/software/spm12/). The 107 regions of interest (ROIs) were obtained using a multiatlas segmentation method (Asman and Landman 2013), while anterior and posterior hippocampi were segmented using FreeSurfer 6 (Fischl 2012), for a total of 111 regions.

fMRI preprocessing

Physiological noise was corrected with RETROICOR (Glover et al. 2000), which was followed by preprocessing with SPM12 that included slice-timing correction, motion correction, normalization to Montreal Neurological Institute (MNI) coordinates, and spatial smoothing with a 6-mm FWHM Gaussian kernel. Next, the mean white matter and cerebrospinal fluid signals, along with the 6 translational and rotational motion parameters were regressed out of the fMRI time courses. The 2 consecutive fMRI scans were then concatenated in time to obtain one 20-min scan. There was no difference in maximum framewise displacement during the scans between the 3 groups as determined by 1-way ANOVA ($P = 0.12$; controls: 1.11 ± 0.94 mm; right mTLE (RmTLE): 1.47 ± 0.77 mm; left mTLE (LmTLE): 1.40 ± 1.01 mm).

FMRI activity (ALFF)

The voxelwise power spectra of the preprocessed fMRI time series were obtained using Welch's method of estimating power spectral density with a Hamming window of length of 120 s and an overlap of 50% (frequency bin width = 8.3 mHz), as opposed to the commonly used Fast Fourier Transform, as Welch's method is less sensitive to noise (Welch 1967). Welch's method uses spectral averaging of frequency spectra obtained from time windowing of the signal to reduce noise and to more accurately approximate the signal in the frequency domain. Since Welch's method requires time windowing, we used a long enough window (120 s) to recover frequencies as low as 0.0083 Hz but short enough to maximize the number of windows to average over for sufficient mitigation of noise. The square root of the power spectrum was then summed over the 0.0083–0.1 Hz band to obtain ALFF (Zang et al. 2007). ALFF was then Z-standardized across gray matter voxels within each subject. We chose to use Z-standardization since it has been shown to remove motion artifacts more effectively than regression

of motion covariates from the fMRI time courses (Yan et al. 2013) as well as having high test–retest reliability (Zuo et al. 2010; Jia et al. 2020).

To obtain frequency-specific ALFF measures, we took the previously obtained power spectra and Z-standardized the square root of the power at each frequency bin across gray matter voxels within each subject. This resulted in 1 ALFF measure per frequency bin (bin width = 8.3 mHz) per subject. Analysis was constrained to frequencies < 0.2 Hz (23 bins in total).

All ALFF metrics of each region were obtained by taking the mean ALFF within the region. Since the fMRI data were collected before and after a scanner upgrade, resulting in different MR signal scales, ALFF metrics were harmonized by linearly regressing out the difference between the 2 groups of data across subjects, while accounting for differences between groups of interest (RmTLE, LmTLE, and controls).

Functional connectivity

FC was obtained by first bandpass filtering the preprocessed fMRI time courses in the 0.0083–0.1 Hz band, then averaging the voxelwise time courses within each region. FC was computed as the Fisher Z-transformed Pearson correlation between each pair of regional time courses.

DWI preprocessing and streamline generation

DWI data were processed according to the PreQual pipeline (Cai et al. 2021), which included denoising (Cordero-Grande et al. 2019), eddy current and motion correction (Andersson and Sotiropoulos 2016), bias correction of B1 field inhomogeneity (Tournier et al. 2019), and synthetic B0 diffusion distortion correction (Schilling et al. 2019). Next, the response function was estimated for spherical deconvolution for the estimation of fiber orientation distribution (Tournier et al. 2007). The gray matter–white matter interface was generated from the T1-weighted and B0 images using SPM12. The 2×10^7 anatomically constrained probabilistic streamlines were generated through the white matter from this interface (Smith et al. 2012) using MRtrix3 (Tournier et al. 2019). The streamlines were then reduced to 1×10^7 using spherical deconvolution-informed filtering of tractograms (SIFT) and then given weights using SIFT2—both of which attempt to better quantify the fiber cross-sectional area (Smith et al. 2015). From this, streamlines connecting each of the 111 ROIs were identified.

White matter fMRI activity connectomes

FMRI data that were corrected for physiological noise (RETROICOR), slice-timing, and motion, but not normalized to MNI coordinates or spatially smoothed, were used for white matter fMRI activity (ALFF) connectome construction. The mean cerebrospinal fluid signal, along with the 6 translational and rotational motion parameters were regressed out of the fMRI time courses and the fMRI data were concatenated to obtain a single 20-min scan. ALFF maps were calculated by taking the square root of the power spectrum in the 0.0083–0.1 Hz band of the fMRI data using Welch's method with the same parameters as above. ALFF maps were then Z-standardized across white matter voxels within each subject.

ALFF maps were registered to the mean B0 diffusion image and were applied to the diffusion MRI-generated streamlines described above to obtain 111 × 111 matrices of the mean ALFF along tracts connecting each pair of gray matter regions. These matrices represent the white matter fMRI activity connectomes. Lastly, group difference dependent on the scanner upgrade was linearly regressed out of white matter fMRI activity connectomes in the same manner as the other ALFF metrics above.

Analysis

Statistical testing of subject demographics and clinical information

Kruskal-Wallis tests were carried out to assess the differences in age and gender between controls, RmTLE patients, and LmTLE patients. Wilcoxon rank-sum tests were carried out to test the differences in clinical parameters between RmTLE and LmTLE patients.

Comparison of fMRI activity between groups

FMRI activity (ALFF) was compared between each group of patients and controls using 2-sample *t*-tests at each region, with significance set at $p_{FWE} < 0.05$ (111 regions). Twenty-six regions were then identified to be used in subsequent analysis as regions that were different between either RmTLE or LmTLE patients and controls as well as their contralateral counterparts in order to include all regions that may be implicated in mTLE.

FMRI activity covariance and associations with mean FC across subjects

ALFF covariance between 2 regions was computed by taking the Pearson correlation between ALFF vectors of the 2 regions, where vector 1 represents the ALFF of region 1 for all *n* subjects and vector 2 represents the ALFF of region 2 for the same *n* subjects. From these, ALFF covariance matrices were constructed by taking the ALFF covariance of each pair of the 26 identified regions within each group (RmTLE, LmTLE, and controls). To test the linear relationship between ALFF covariance and FC, ALFF covariance values were compared to mean FC values across subjects in each group at each edge of the 26 × 26 matrix (325 edges) using Spearman correlations. Two separate correlations were run within each group, i.e. edges where the ALFF correlation was >0, and edges where the ALFF correlation was ≤0. To obtain *P*-values for the correlations, a null distribution of Spearman correlation coefficients was built for each of the correlations run by randomly permuting the ALFF covariance and FC values 10,000 times.

Comparison of white matter fMRI activity between groups

White matter fMRI activity connectomes were reduced to the 26 identified regions used in the previous analysis, and 2-sample *t*-tests were performed at each edge between RmTLE patients and controls as well as between LmTLE patients and controls. Note: 1 RmTLE patient and 1 control subject did not undergo DWI and were thus excluded from the white matter fMRI activity analysis.

Testing the dependence of the fMRI activity increases on specific regions

We then aimed to determine the dependence of the group differences on the ALFF of the anterior hippocampus ipsilateral to the epileptic side (the presumed focus). To test this, the ALFF of the ipsilateral anterior hippocampus was linearly regressed out of the ALFF of all other regions across subjects. Then, 2-sample *t*-tests between patients and controls were performed at each region previously found to be significant using the same significance threshold as previously ($P < 0.05/111$ regions). Next, we sought to determine whether the ALFF increases in other regions could explain the ALFF increase in the anterior hippocampus as a control for the above analysis. The previous procedure was repeated but with linearly regressing out the ALFF of all the other previously identified regions with increased ALFF, aside from the ipsilateral anterior hippocampus, using 2 different methods. We first built a multiple linear regression model to control for all increased ALFF regions at once, then tested the differences between patients and controls. Due to possible confounds of multicollinearity between predictors in this multiple linear regression model, we then built regression models for each one of these increased ALFF regions individually and tested the differences between patients and controls after each of these regressions.

Relating fMRI activity to clinical metrics

The ipsilateral anterior hippocampus ALFF change from controls was quantified as the ALFF difference from the control mean in the right anterior hippocampus in RmTLE patients and as the ALFF difference from the control mean in the left anterior hippocampus in LmTLE patients. This change was correlated with the duration of disease using a Spearman correlation. Next, this change was compared between patients with and without MTS identified by MRI as well as between patients with and without presence of focal-to-bilateral tonic-clonic seizures (FBTCS) using 2-sample *t*-tests.

The decreases in ALFF seen in RmTLE patients were quantified as the difference from the control mean and were compared to the duration of disease using a Spearman correlation. These decreases were also compared between patients with and without MTS identified by MRI as well as between patients with and without presence of FBTCS using 2-sample *t*-tests. This was performed only in RmTLE patients since no ALFF decreases were detected in LmTLE patients. Significance was set at $p_{FWE} < 0.05$ for the comparisons of ALFF of these 7 regions with the clinical metrics. Note: 1 subject in the RmTLE group reported an unknown age of onset in their childhood, so they were not included in any duration correlational analyses.

Comparison of frequency-specific ALFF between groups

Frequency-specific ALFF at each of the 26 identified regions was compared between each group of patients and controls at each frequency bin using 2-sample *t*-tests with false-discovery rate (FDR) correction for the number of frequency bins (23 bins).

Results

Subject demographic and clinical characteristics

There were no differences found in any of the demographic characteristics tested between RmTLE, LmTLE, and controls (Table 1). The only difference in clinical characteristics was a higher percentage of LmTLE patients with MTS on MRI than RmTLE patients ($P < 0.05$, Table 1).

FMRI activity alterations in mTLE

In RmTLE patients, increases in ALFF were found in the bilateral anterior hippocampi, bilateral posterior hippocampi, right amygdala, right entorhinal cortex, right parahippocampal gyrus, right inferior temporal gyrus, right temporal pole, bilateral ventral diencephalon, and the right basal forebrain compared to controls ($p_{FWE} < 0.05$, Fig. 1a). In LmTLE patients, increases in ALFF were found in bilateral anterior hippocampi and in the right ventral diencephalon compared to controls ($p_{FWE} < 0.05$, Fig. 1b). The most significant increases were in the anterior hippocampus ipsilateral to the epileptic side in both groups. Decreases in ALFF were found in multiple nodes of the DMN in RmTLE patients, i.e. the right medial superior frontal gyrus (MSFG), bilateral posterior cingulate cortex (PCC), bilateral precunei, and bilateral angular gyri ($p_{FWE} < 0.05$, Fig. 1a). No decreases in ALFF were found in LmTLE patients. The union of regions with altered ALFF in both groups of mTLE patients as well as their contralateral counterparts (26 regions total) were then identified to be used in the subsequent analyses.

FMRI activity covariance and association with FC

We next evaluated the covariance of ALFF between regions across subjects to probe whether the ALFF changes in different regions were related. We constructed covariance matrices by calculating the Pearson correlation of ALFF across subjects between the 26 regions mentioned above. Positive ALFF covariance indicates coupling of signal power changes across subjects, whereas negative ALFF covariance indicates that an increase in power of 1 region corresponds to a decrease in

Table 1. Subject demographics and clinical information.

	RmTLE ($n = 32$)	LmTLE ($n = 15$)	Controls ($n = 96$)	*P*-value
Age (years)	41.1 ± 11.7	37.1 ± 14.4	37.9 ± 13.4	0.34[a]
Gender (M/F)	15/17	10/5	50/46	0.45[a]
Duration of epilepsy (years)	20.0 ± 15.0[b]	23.2 ± 16.7		0.51[c]
MTS on MRI	19 (59%)	14 (93%)		0.02[d,c]
MTS or mesial temporal gliosis from pathology	28 (97%)[e]	14 (100%)[f]		0.51[c]
PET hypometabolism localization	27 (84%)	12 (80%)		0.72[c]
Interictal EEG localization	26 (81%)	9 (60%)		0.13[c]
Ictal EEG localization	27 (84%)	14 (93%)		0.41[c]
Had SEEG study	4 (13%)	0 (0%)		0.16[c]
Presence of FBTCS	15 (47%)	10 (67%)		0.22[c]

[a]Kruskal-Wallis test. [b]One RmTLE patient's duration of epilepsy is unknown and was not included ($n = 31$). [c]Wilcoxon rank-sum test. [d]$P < 0.05$. [e]Three RmTLE patients did not have a postoperative pathology specimen ($n = 29$). [f]One LmTLE patient did not have a postoperative pathology specimen ($n = 14$).

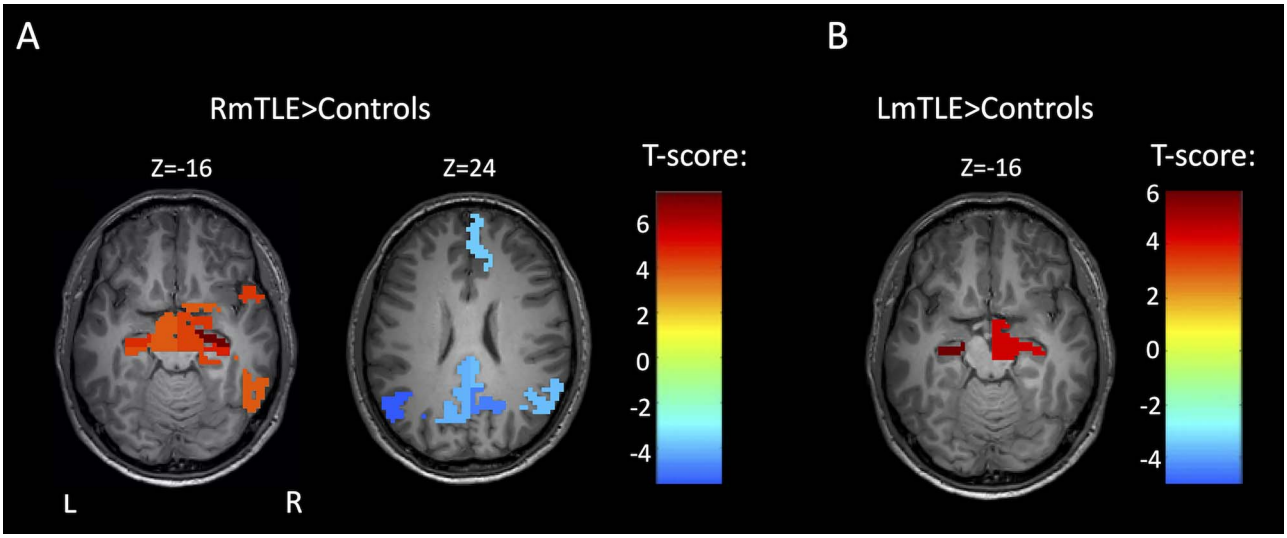

Fig. 1. FMRI activity changes in mTLE. a) Regionwise comparison of ALFF between RmTLE patients ($n = 32$) and controls ($n = 96$). b) Regionwise comparison of ALFF between and LmTLE patients ($n = 15$) and controls ($n = 96$). Maps are thresholded at $p_{FWE} < 0.05$, 2-sample *t*-test.

power in another region. There was significant positive covariance in ALFF within and across temporal lobes as well as within DMN regions in controls ($p_{unc} < 0.05$, Fig. 2a). MTLE patients showed overall similar covariance patterns to controls. Interestingly, there was significant positive ALFF covariance in a small core of ipsilateral mesial temporal regions, i.e. the anterior hippocampus, amygdala, parahippocampal gyrus, and entorhinal cortex in both RmTLE and LmTLE groups (red boxes, $p_{unc} < 0.05$, Fig. 2b and c). RmTLE patients had positive covariance between the ALFF of right and left mesial temporal regions similar to controls ($p_{unc} < 0.05$, Fig. 2b). Both groups of mTLE patients had negative covariance between the ALFF of a few temporal and DMN regions ($p_{unc} < 0.05$, Fig. 2b and c). Notably, there was negative ALFF covariance between the right inferior temporal gyrus and the bilateral PCC and precunei in RmTLE patients as well as between the right inferior temporal gyrus and the bilateral precunei and left angular gyrus in LmTLE patients ($p_{unc} < 0.05$, Fig. 2b and c).

Mean FC matrices between each pair of the 26 regions have a similar overall structure to the ALFF covariance matrices. By visual inspection, the mesial temporal regions with strong ALFF covariance are also highly functionally connected (Fig. 2d–f). Along with these qualitative observations, there is a strong association of positive ALFF covariance and mean FC between regions across each group (controls: $r_{spearman} = 0.74$, $P < 0.0001$; RmTLE: $r_{spearman} = 0.59$, $P < 0.0001$; LmTLE: $r_{spearman} = 0.51$, $P < 0.0001$; permutation test; Fig. 2g–i).

White matter fMRI activity alterations in mTLE

Next, we evaluated the ALFF changes in mTLE along white matter tracts connecting the 26 regions. At the corrected level, the only changes in white matter ALFF were an increase in ALFF along tracts connecting the right anterior and posterior hippocampus and a decrease in ALFF along tracts connecting the right precuneus and PCC in RmTLE patients ($p_{FWE} < 0.05$, Fig. 3a). There were no changes in white matter ALFF detected in LmTLE patients at the corrected level. At the uncorrected level, tracts connecting ipsilateral temporal and subcortical regions (red solid boxes) had increased ALFF in both

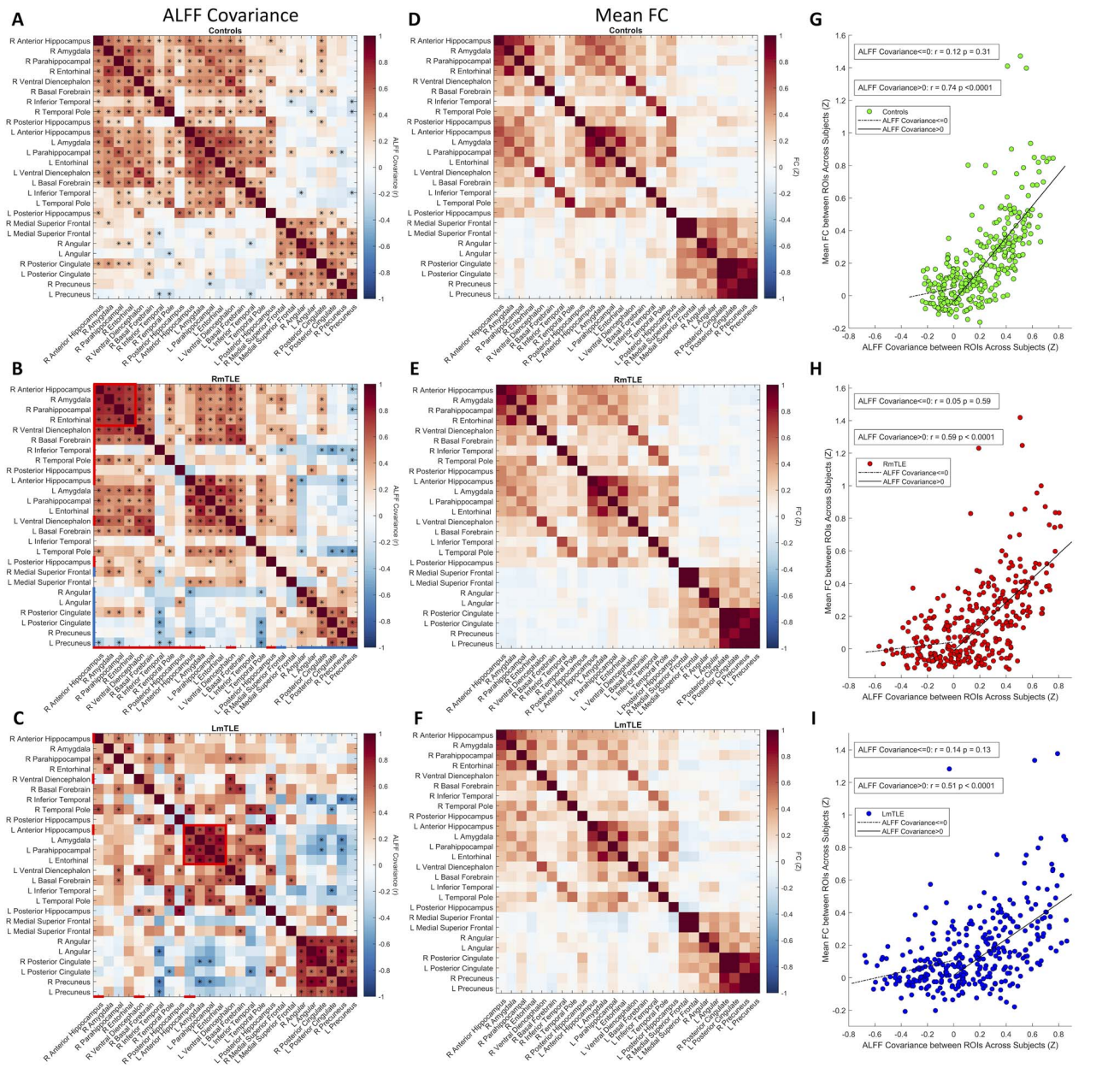

Fig. 2. Regional fMRI activity covariance across subjects and association with FC. a–c) Regionwise ALFF covariance matrices across subjects in 26 identified regions for controls ($n = 96$), RmTLE patients ($n = 32$), and LmTLE patients ($n = 15$), respectively, calculated by Pearson correlation ($^{*}p_{\mathrm{unc}} < 0.05$). Regions with ALFF increases are denoted with red lines and regions with ALFF decreases are denoted with blue lines on left and bottom edges of ALFF covariance matrices. Red boxes highlight a small core of ipsilateral mesial temporal regions with positive ALFF covariance in both RmTLE and LmTLE patients. (d–f) Mean FC matrices in the 26 regions across each group for controls, RmTLE patients, and LmTLE patients. (g–i) Scatter plots of ALFF correlations between regions and mean FC between regions across subjects for all pairs of the 26 regions for controls, RmTLE patients, and LmTLE patients, with each point representing a single edge. Spearman correlations are shown on each plot between mean FC and ALFF covariance for ALFF covariance > 0 and ALFF covariance ≤ 0 separately. There is a strong association between the ALFF correlation and mean FC in pairs of nodes with a positive ALFF covariance for all 3 groups (spearman correlation, $P < 0.0001$, permutation test). R: right; L: left.

groups ($p_{\mathrm{unc}} < 0.05$, Fig. 3a and b) and tracts connecting contralateral temporal and subcortical regions (red dashed boxes) had increased ALFF in LmTLE patients. Decreases in ALFF at the uncorrected level were found along tracts connecting DMN regions (blue boxes) in RmTLE patients ($p_{\mathrm{unc}} < 0.05$, Fig. 3a) and a few tracts connecting temporal and subcortical regions to DMN regions (green boxes) in both RmTLE and LmTLE patients ($p_{\mathrm{unc}} < 0.05$, Fig. 3a and b).

FMRI activity alterations in mTLE controlling for the effects of certain regions

To address whether the ipsilateral anterior hippocampus (presumed epileptic focus) may be the primary region of the increased fMRI activity, we tested whether the ALFF changes in other regions were dependent on the ALFF of the ipsilateral anterior hippocampus. This was carried out by linearly regressing out the ALFF of the ipsilateral anterior hippocampus from the ALFF of other

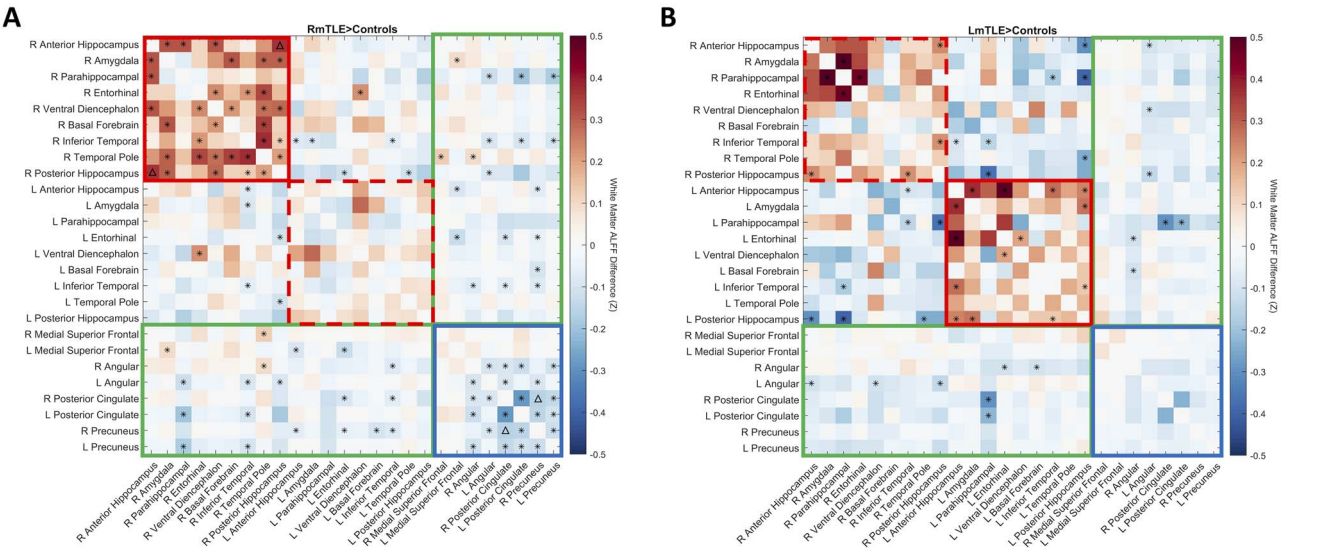

Fig. 3. FMRI activity changes along white matter tracts in mTLE. Mean differences in ALFF along white matter tracts are shown between RmTLE patients ($n = 31$) and controls ($n = 95$) a) and between LmTLE patients ($n = 15$) and controls ($n = 95$) b) between the 26 identified regions. Red solid boxes denote tracts connecting ipsilateral temporal and subcortical regions; red dashed boxes denote tracts connecting contralateral temporal and subcortical regions; blue boxes denote tracts connecting DMN regions; green boxes denote tracts connecting temporal and subcortical to DMN regions. $^{*}p_{unc} < 0.05$, $\Delta p_{FWE} < 0.05$, 2-sample t-test. R: right; L: left.

regions and by retesting the differences between patients and controls in regions that were previously found to have differences. We found that the only remaining significant differences between RmTLE patients and controls were decreases in nodes of the DMN, i.e. the right MSFG, bilateral PCC, right precuneus, and bilateral angular gyri, with no remaining ALFF increases ($p_{FWE} < 0.05$, Fig. 4a). No significant differences remained in the right VDC or right anterior hippocampus of LmTLE patients. We then tested whether the increase in the ALFF of the ipsilateral anterior hippocampus was dependent on the ALFF of other regions with increased ALFF. To evaluate this, we repeated the previous analysis, but linearly regressed out the ALFF of all other regions with increased ALFF (excluding the ipsilateral anterior hippocampus) in each of the groups: RmTLE—the left anterior hippocampus, bilateral posterior hippocampi, right amygdala, right entorhinal cortex, right parahippocampal gyrus, right inferior temporal gyrus, right temporal pole, bilateral ventral diencephalon, and the right basal forebrain; LmTLE—the right anterior hippocampus and right ventral diencephalon. After regressing out the ALFF of all these regions using a multiple linear regression model, there was still a significant increase between RmTLE patients and controls in the right anterior hippocampus and significant decreases in the right MSFG, bilateral PCC, right precuneus, and bilateral angular gyri ($p_{FWE} < 0.05$, Fig. 4b). After controlling for the ALFF of these regions in LmTLE patients, there was still a significant increase in the ALFF of the left anterior hippocampus ($p_{FWE} < 0.05$). When regressing out each of these increased ALFF regions individually, the ipsilateral anterior hippocampus remained significantly different between mTLE patients and controls in all cases (Supplementary Fig. S1).

FMRI activity correlations with clinical metrics

We compared the ALFF increase from the control mean of the ipsilateral anterior hippocampus to disease duration, presence of MTS on MRI, and presence of FBTCS. The ipsilateral anterior hippocampus ALFF change was increased in patients with MTS on MRI ($p_{unc} = 0.02$, 2 sample t-test, Fig. 5a), trended lower in patients with FBTCS ($p_{unc} = 0.07$, 2 sample t-test, Fig. 5b), and was positively correlated with disease duration ($r_{spearman} = 0.33$, $p_{unc} = 0.03$, Fig. 5c).

We next related the ALFF change from the control mean of the regions with decreased ALFF in RmTLE patients (right MSFG, bilateral PCC, bilateral precunei, and bilateral angular gyri) to clinical metrics. The ALFF change of the right MSFG had a negative trend with disease duration ($r_{spearman} = -0.47$, $p_{FWE} = 0.05$, Fig. 5d); however, none of the other regions were related to disease duration in RmTLE patients. No relationships were found between ALFF of these regions and MTS on MRI nor the presence of FBTCS in RmTLE patients.

Frequency-specific fMRI activity alterations in mTLE

While the analyses above used the conventional ALFF, a summed amplitude over a frequency range, we next assessed the frequency specificity of these ALFF changes by probing the amplitude at each frequency bin in the 26 identified regions used in the analyses above, resulting in frequency-specific ALFF. The majority of regions with increased ALFF in mTLE patients had increases in frequency-specific ALFF across the conventional ~0–0.1 Hz band. In a few regions, namely the bilateral anterior hippocampi, right inferior temporal gyrus and bilateral temporal pole of RmTLE patients and the left anterior hippocampus, right basal forebrain, right

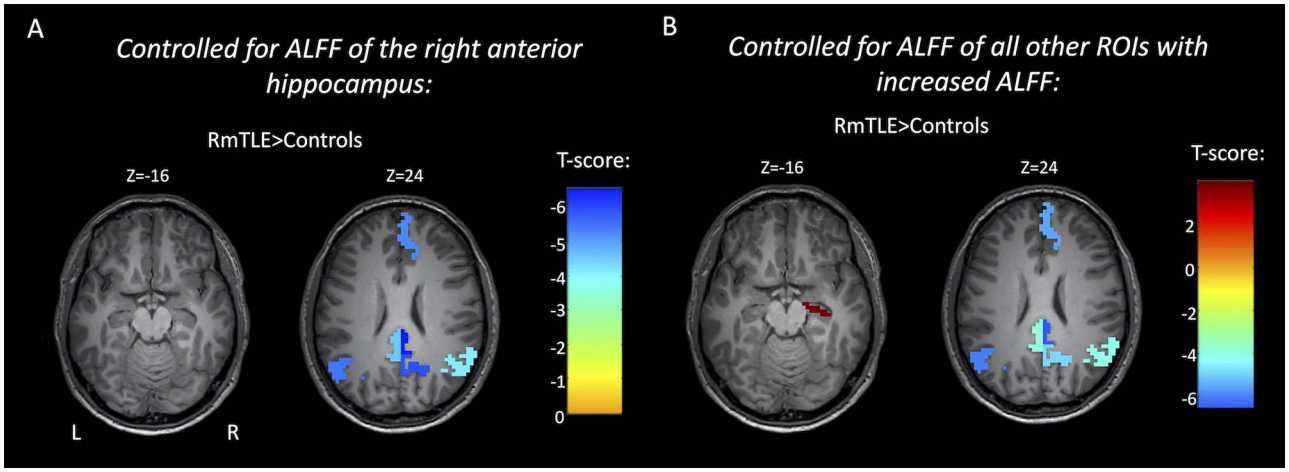

Fig. 4. FMRI activity increases in mTLE are dependent on the fMRI activity of the ipsilateral anterior hippocampus. Regionwise comparison of ALFF between RmTLE patients ($n = 32$) and controls ($n = 96$) in regions with previously shown significant group differences after controlling for the ALFF of the right anterior hippocampus a) and after controlling for the ALFF of all other regions that had increased ALFF in RmTLE patients (excluding the ipsilateral anterior hippocampus) b). Maps are thresholded at $p_{FWE} < 0.05$.

inferior temporal gyrus, and bilateral temporal pole of LmTLE patients, these ALFF increases extended into frequencies > 0.1 Hz ($p_{FDR} < 0.05$, Fig. 6). RmTLE patients had frequency-specific ALFF decreases in the right MSFG and the bilateral angular gyri across the conventional low-frequency band (~0–0.1 Hz) that extended slightly >0.1 Hz; however, there were no differences in these regions in LmTLE patients. RmTLE patients had decreases in frequency-specific ALFF across the entire frequency band (~0–0.2 Hz) in the bilateral PCC and precunei. LmTLE patients had decreases in frequency-specific ALFF across the ~0.05–0.2 Hz band in these same regions ($p_{FDR} < 0.05$, Fig. 6).

Discussion

In this study, we identified increased fMRI activity (ALFF) in a network of temporal and subcortical regions of patients with mTLE. We then provided evidence that these epileptic fMRI activity increases are potentially spreading throughout this network along both functional and structural connections and likely originate in the epileptic focus. Furthermore, we found that the increased fMRI activity of the focus may be related to disease severity and progression. We also show fMRI activity decreases in the DMN regions in RmTLE patients, with evidence that they may originate from a different mechanism than the reported ALFF increases.

FMRI activity increases and spread

Increases in ALFF were found across the temporal and subcortical structures in mTLE patients. The most significant of these increases was in the epileptic anterior hippocampus in both RmTLE and LmTLE patients. These increases both aligned with prior reports of ALFF in mTLE (Zhang et al. 2010, 2015), as well as provided evidence that these ALFF alterations have pathological underpinnings, given their localization to the epileptic focus.

Because of this, we hypothesized that the signals causing this increased fMRI activity originate in the focus and spread throughout the epileptic network. To address this hypothesis, we showed that the regions of increased ALFF had strong positive covariance across subjects using a method similar to that used to identify structural covariance networks. We then showed that this covariance was positively related to FC, suggesting that the increased ALFF may be spreading through a functional network. However, this association between ALFF covariance and FC was somewhat anticipated, as functionally connected regions are expected to share changes in signal power. Next, we detected ALFF increases along white matter tracts connecting the same network of regions in both RmTLE and LmTLE patients. However, it should be noted that most of these white matter ALFF changes were only found without correcting for multiple comparisons; hence, these results should be interpreted qualitatively. Last, we found that the measured increases in fMRI activity were linearly dependent on the ipsilateral anterior hippocampus, the presumed epileptic focus, but that the increase in the fMRI activity of this focus was not dependent on the other regions with increased fMRI activity. This indicates that the epileptic focus is the region of primary activity alterations but that the epileptic activity is not spreading uniformly to the rest of the network. Taken together, these data imply epileptic fMRI activity increases in the seizure focus that potentially spread across a network of temporal and subcortical regions.

There are well-known connections between many of the regions in the network identified in this study, namely, the hippocampi, amygdalae, parahippocampal regions, and entorhinal cortex as a part of the hippocampal-diencephalic-cingulate network, which is also known as the Papez circuit (Bubb et al. 2017). The hippocampal commissure also connects the 2 hippocampi and has been suggested as a route for ipsilateral to contralateral mesial temporal seizure spread

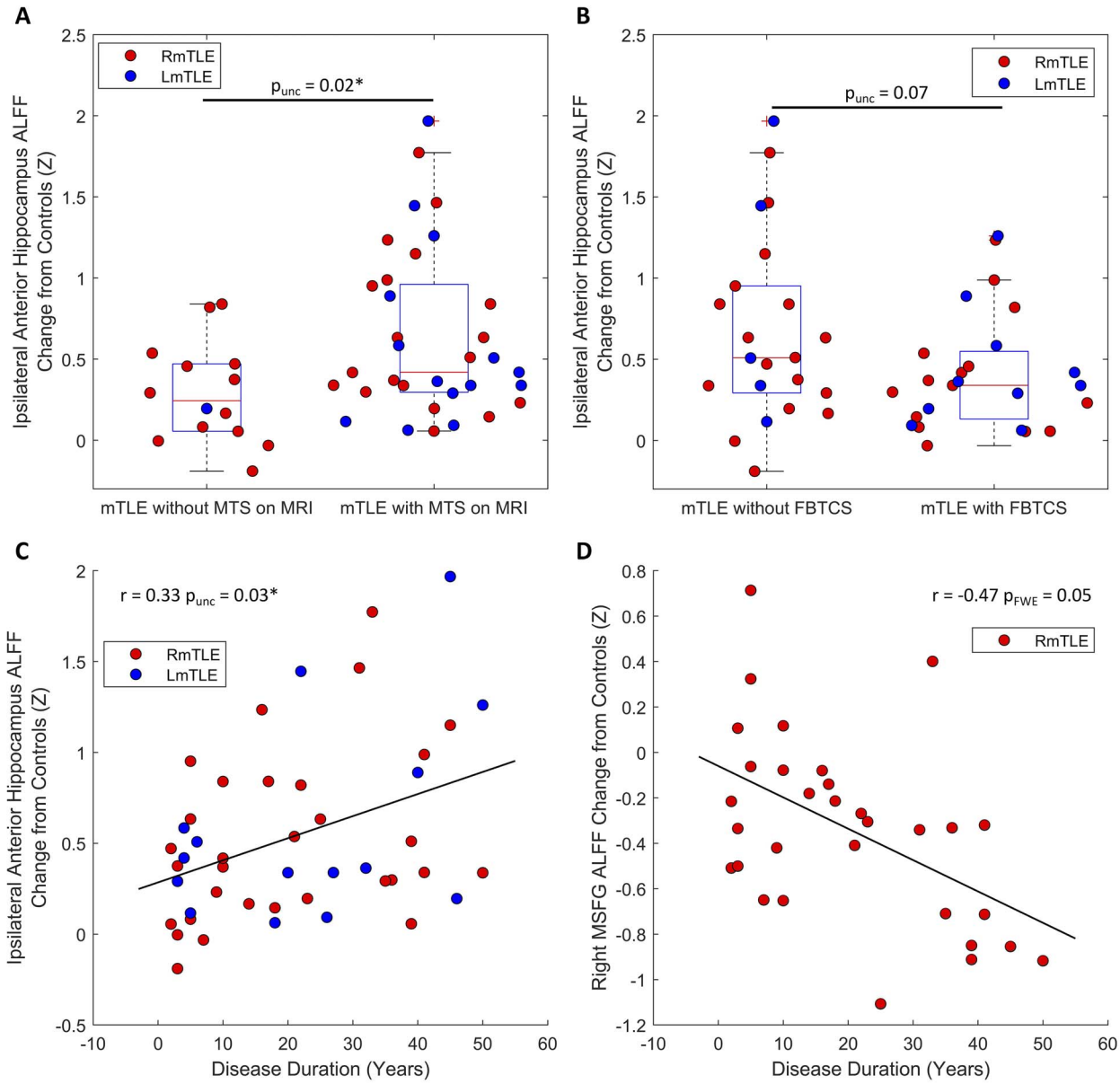

Fig. 5. FMRI activity changes are related to disease severity and progression in mTLE. a) Patients with evidence of MTS on MRI ($n = 33$) have a higher ALFF increase from controls in their ipsilateral anterior hippocampus than patients without evidence of MTS on MRI ($n = 14$) ($p_{unc} = 0.02$, 2-sample t-test). b) The ipsilateral anterior hippocampus ALFF increase from controls trends higher in patients without FBTCS ($n = 22$) than patients with FBTCS ($n = 25$); however, there is no significant difference ($p_{unc} = 0.07$, 2-sample t-test). c) The ipsilateral anterior hippocampus ALFF change from controls tends to increase with disease duration in mTLE patients ($r_{spearman} = 0.33$, $p_{unc} = 0.03$, $n = 46$). d) Right MSFG ALFF change from controls has a trend toward a decrease as the disease progresses in RmTLE patients ($r = -0.47$, $p_{FWE} = 0.05$, $n = 31$). $^{*}p < 0.05$. MTS: mesial temporal sclerosis.

(Gloor et al. 1993). These known anatomical connections provide evidence for the structural pathways of fMRI activity spread between many of the temporal and subcortical regions in this study.

Pathophysiological origins of fMRI activity increases

The increase in fMRI activity in the epileptic focus was found to increase with the duration of epilepsy and was higher in patients with MTS identified on MRI, implying an association with a more severe, progressed disease. We did not find a significant relationship between the fMRI activity of the focus and history of FBTCS. Similarly, previous work has failed to find a significant association between history of FBTCS and progression of mTLE (Bernasconi et al. 2005).

Zhang et al. proposed interictal spiking as a possible neurophysiological basis for the ALFF increases in mTLE, given that a correlation was found between the ALFF of ipsilateral mesial temporal structures and interictal spiking (Zhang et al. 2010). Furthermore, multiple studies have found that the fMRI signal increases in the epileptic focus during interictal spikes (Salek-Haddadi et al. 2006;Laufs et al. 2007 ; Kobayashi et al. 2009), providing

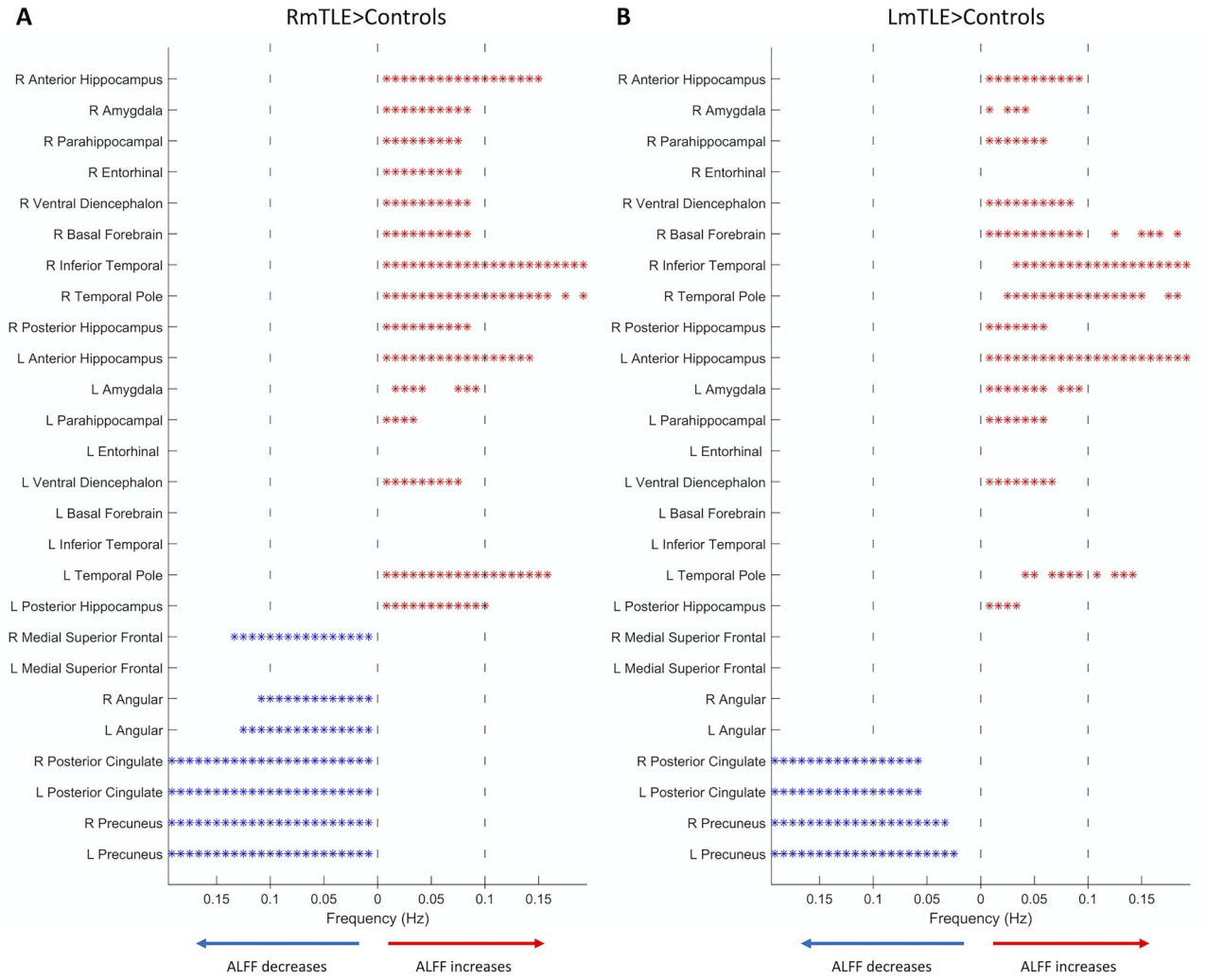

Fig. 6. Frequency-specific fMRI activity changes in mTLE. Significant differences in frequency-specific ALFF between RmTLE patients ($n = 32$) and controls ($n = 96$) A) and LmTLE patients ($n = 15$) and controls ($n = 96$) B) in the 26 identified regions in the same order as in previous figures. Significant differences at each frequency bin are indicated by an asterisk, with increases to the right in red and decreases to the left in blue. Vertical dashed lines denote the typical frequency band used in fMRI (~0–0.1 Hz). $^{*}p_{FDR} < 0.05$ (23 frequency bins), 2-sample t-test. R: right; L: left.

additional evidence that interictal spiking increases fMRI signal power in the epileptic focus. Additionally, Beers et al. used concurrent intracranial EEG–fMRI and found that interictal spikes in the mesial temporal regions elicited fMRI signal increases with durations of ~5–12.5 s, which corresponds to frequencies of ~0.04–0.1 Hz (Beers et al. 2015). These frequencies correspond well to the frequencies in which we found increased ALFF in mesial temporal regions, which bolsters the hypothesis that these increases in ALFF are arising from the hemodynamic response to interictal spiking. Tang et al. also recently found that the regions identified as epileptic foci using increased ALFF as a biomarker were highly concordant with the regions identified using ictal intracranial EEG (Tang et al. 2021), providing further evidence for a neurophysiological origin of fMRI activity increases in focal epilepsy. Another recent study showed that, like electrical activity, fMRI activity can spread during interictal spikes (Kowalczyk et al. 2020), which could be related to the potential spread of epileptic fMRI activity observed in this study.

FMRI activity decreases in DMN regions

The finding that ALFF was decreased in the DMN regions in RmTLE patients is consistent with prior studies (Zhang et al. 2010, 2015; Wei et al. 2016). Decreases in ALFF were also found along white matter tracts between DMN regions in RmTLE patients. This decreased activity propagation throughout the network could be related to previous reports of fMRI abnormalities in the DMN of mTLE patients (Liao et al. 2011; Haneef et al. 2012). The ALFF change of the right MSFG had a negative trend with epilepsy duration in RmTLE patients; however, no other regions with decreases had any relationship with the clinical metrics tested. Multiple studies have demonstrated fMRI deactivations in the PCC, a primary node of the DMN, during interictal spikes (Laufs et al. 2007; Kobayashi et al. 2009), which could explain the

suppressed DMN activity we found in RmTLE patients. However, if interictal spiking was responsible for the ALFF changes in both regions with ALFF increases and decreases, we would expect to see stronger negative ALFF covariance between these 2 sets of regions. Previous studies using fMRI have also shown that the DMN is suppressed and decoupled during sleep (Horovitz et al. 2009; Sämann et al. 2011) and that ALFF and FC within the DMN are decreased in the eyes-closed compared to the eyes-opened condition (Yan et al. 2009), all suggesting that the activity and connectivity of the DMN are decreased in lower states of consciousness. There has been growing evidence that mTLE patients have impaired consciousness and arousal modulating networks (Englot et al. 2020), suggesting that the decreases in DMN ALFF reported here may be due to altered consciousness in mTLE. However, further evidence would be required to support this claim.

Frequency specificity of fMRI activity alterations

The frequency specificity of the fMRI activity changes in mTLE patients revealed differing patterns for the regions with increased and those with decreased activity. ALFF increases were primarily in the typical low-frequency band used in fMRI analyses (~0–0.1 Hz) with a few regions showing increases in higher frequencies (>0.1 Hz). This suggests that the increased fMRI activity may primarily spread throughout these lower frequencies. Increases in power of the fMRI signal have previously been reported in the anterior nucleus and pulvinar of the thalamus in very low frequencies (~0–0.032 Hz) in TLE patients (Morgan et al. 2015). The anterior nucleus is one of the main nodes in the hippocampal-diencephalic-cingulate network described above, which further supports our evidence of increased low-frequency fMRI activity spread throughout this network.

On the other hand, the frequencies of ALFF decreases varied. In the right MSFG and angular gyri, decreases manifested in the lower frequencies in RmTLE patients. The PCC and precunei were decreased across the full frequency band (~0–0.2 Hz) in RmTLE patients and most of the full band in LmTLE patients, possibly suggesting different underpinnings than the right MSFG and angular gyri. This may be linked to decoupling of the anterior and posterior DMN previously reported in mTLE (Haneef et al. 2012). The finding of ALFF changes >0.1 Hz in these regions also bolsters the evidence that there is interesting information in the fMRI signal above the typical cutoff of 0.1 Hz, as suggested by previous studies (Chen and Glover 2015; Gohel and Biswal 2015); however, we cannot be sure what the origins of the different frequencies are in this study.

Links between fMRI activity increases and decreases

While we showed that the fMRI activity increases and decreases have different characteristics, there are some interesting potential links between these 2 sets of regions specifically between the right inferior temporal gyrus and the DMN. We found both negative ALFF covariance and ALFF decreases in the white matter connecting these regions, which could indicate an inhibitory connection. There are also known connections between mesial temporal structures and both the PCC (Bubb et al. 2017) and the precuneus (Jitsuishi and Yamaguchi 2021), the 2 main nodes of the DMN. However, the decreases in ALFF in all of these regions but the left precuneus were independent of the increases in ALFF, as shown by the regression analysis, reducing confidence that the decreases in the DMN are directly linked to spread from the temporal and subcortical regions.

Notable differences between FC and ALFF covariance

In this study, we presented a metric we termed "ALFF covariance," i.e. the Pearson correlation of ALFF for each pair of regions across subjects. This metric is similar to FC in that it assesses the correspondence of 2 regional signals, implying connectivity between those regions. However, whereas the conventional computation of FC (0-lag Pearson correlation) is dependent on the phase of the 2 signals and on a linear temporal relationship between the 2 signals, ALFF covariance is not dependent on either of these. Because ALFF is merely a quantification of signal power, the covariance of this metric across subjects is phase-independent and allows for nonlinear temporal relationships between signals. ALFF covariance instead relies upon a linear relationship between signal power in the 2 regions across subjects. For example, 2 signals could both be both 0-lag uncorrelated and have no apparent lagged linear relationship. These signals would not have a high FC, lagged or not. However, if the power of these 2 signals increased across subjects together, they would have a high positive ALFF covariance. We can empirically see something like this in the scatterplots of ALFF covariance and mean FC, where pairs of regions with a negative ALFF covariance effectively have an FC of 0. This is likely due to a relationship between the 2 regional signals that FC is not sensitive to. However, since ALFF covariance is computed across a group of subjects, it is unavailable at the individual level.

Limitations

One limitation of this study is the lack of concurrent electrophysiological recordings with the fMRI data to inform the electrophysiological correlates of the fMRI signal activity and spread observed. These data were also collected interictally, and the relationship between ictal and interictal electrographic and fMRI progression could not be determined. Another limitation is the small number of subjects in each of the patient groups, leading to reduced power, particularly with regard to the LmTLE group. While it would be possible to combine these 2 groups, numerous studies have shown that LmTLE and RmTLE patients have distinct network alterations (Ahmadi et al. 2009; Besson et al. 2014;

de Campos et al. 2016). The findings of statistically significant ALFF changes along white matter tracts were also fairly sparse and most differences were only found prior to multiple comparison correction. This study also did not assess how dynamic changes in fMRI signals corresponded to the ALFF alterations found. Further studies using high temporal resolution fMRI may be able to link the spread of dynamic activity to further infer the causal dynamics of the spread. The epileptic foci of these patients were also identified through presurgical workup and were not verified based on surgical outcomes or other data. Lastly, no analyses considered the effects of antiepileptic medications.

Conclusion

In this study, we identified increased low-frequency fMRI activity in the epileptic focus and connected regions in mTLE. We provided evidence that these epileptic fMRI activity increases were potentially spreading through a temporal and subcortical epileptic network from the focus across a specific low-frequency band. Moreover, we found that fMRI activity in the focus may increase with disease severity and progression in mTLE. We also identified fMRI activity decreases in the DMN of RmTLE patients and provided evidence that they may have a different pathophysiological origin than the activity increases in the focus. Taken together, this work provides an important link between fMRI and potential resting epileptic activity propagation across the brain, which might inform seizure onset localization and progression. Furthermore, this work may contribute to the understanding of the basic properties of the fMRI signal which produce the resting brain network alterations reported in mTLE and focal epilepsy.

Supplementary material

Supplementary material is available at *Cerebral Cortex* online.

Funding

This work was supported by the National Institute of Biomedical Imaging and Bioengineering at the National Institutes of Health (T32EB021937 to L.E.S.) and the National Institute of Neurological Disorders and Stroke at the National Institutes of Health (R01 NS075270, R01 NS108445, and R01 NS110130 to V.L.M.; R00 NS097618 to D.J.E.).

Conflict of interest statement. None declared.

Data Availability Statement

Data and algorithms that support this study are available upon reasonable request to the corresponding author.

References

Ahmadi ME, Hagler DJ, McDonald CR, Tecoma ES, Iragui VJ, Dale AM, Halgren E. Side matters: diffusion tensor imaging tractography in left and right temporal lobe epilepsy. *Am J Neuroradiol*. 2009:30:1740–1747.

Andersson JLR, Sotiropoulos SN. An integrated approach to correction for off-resonance effects and subject movement in diffusion MR imaging. *NeuroImage*. 2016:125:1063–1078.

Asman AJ, Landman BA. Non-local statistical label fusion for multi-atlas segmentation. *Med Image Anal*. 2013:17:194–208.

Beers CA, Williams RJ, Gaxiola-Valdez I, Pittman DJ, Kang AT, Aghakhani Y, Pike GB, Goodyear BG, Federico P. Patient specific hemodynamic response functions associated with interictal discharges recorded via simultaneous intracranial EEG-fMRI. *Hum Brain Mapp*. 2015:36:5252–5264.

Bernasconi N, Natsume J, Bernasconi A. Progression in temporal lobe epilepsy: differential atrophy in mesial temporal structures. *Neurology*. 2005:65:223–228.

Besson P, Dinkelacker V, Valabregue R, Thivard L, Leclerc X, Baulac M, Sammler D, Colliot O, Lehéricy S, Samson S, et al. Structural connectivity differences in left and right temporal lobe epilepsy. *NeuroImage*. 2014:100:135–144.

Bettus G, Guedj E, Joyeux F, Confort-Gouny S, Soulier E, Laguitton V, Cozzone PJ, Chauvel P, Ranjeva J-P, Bartolomei F, et al. Decreased basal fMRI functional connectivity in epileptogenic networks and contralateral compensatory mechanisms. *Hum Brain Mapp*. 2009:30:1580–1591.

Bettus G, Bartolomei F, Confort-Gouny S, Guedj E, Chauvel P, Cozzone PJ, Ranjeva J-P, Guye M. Role of resting state functional connectivity MRI in presurgical investigation of mesial temporal lobe epilepsy. *J Neurol Neurosurg Psychiatry*. 2010:81:1147–1154.

Bubb EJ, Kinnavane L, Aggleton JP. Hippocampal–diencephalic–cingulate networks for memory and emotion: an anatomical guide. *Brain Neurosci Adv*. 2017:1:2398212817723443.

Cai LY, Yang Q, Hansen CB, Nath V, Ramadass K, Johnson GW, Conrad BN, Boyd BD, Begnoche JP, Beason-Held LL, et al. PreQual: an automated pipeline for integrated preprocessing and quality assurance of diffusion weighted MRI images. *Magn Reson Med*. 2021:86:456–470.

Chen JE, Glover GH. BOLD fractional contribution to resting-state functional connectivity above 0.1Hz. *NeuroImage*. 2015:107:207–218.

Cordero-Grande L, Christiaens D, Hutter J, Price AN, Hajnal JV. Complex diffusion-weighted image estimation via matrix recovery under general noise models. *NeuroImage*. 2019:200:391–404.

Davis KA, Jirsa VK, Schevon CA. Wheels within wheels: theory and practice of epileptic networks. *Epilepsy Curr*. 2021:21:243–247.

de Campos BM, Coan AC, Lin Yasuda C, Casseb RF, Cendes F. Large-scale brain networks are distinctly affected in right and left mesial temporal lobe epilepsy. *Hum Brain Mapp*. 2016:37:3137–3152.

Ding Z, Huang Y, Bailey SK, Gao Y, Cutting LE, Rogers BP, Newton AT, Gore JC. Detection of synchronous brain activity in white matter tracts at rest and under functional loading. *Proc Natl Acad Sci*. 2018:115:595–600.

Englot DJ, D'Haese P-F, Konrad PE, Jacobs ML, Gore JC, Abou-Khalil BW, Morgan VL. Functional connectivity disturbances of the ascending reticular activating system in temporal lobe epilepsy. *J Neurol Neurosurg Psychiatry*. 2017:88:925–932.

Englot DJ, Morgan VL, Chang C. Impaired vigilance networks in temporal lobe epilepsy: mechanisms and clinical implications. *Epilepsia*. 2020:61:189–202.

Fischl B. FreeSurfer. *NeuroImage*. 20 YEARS OF fMRI. 2012:62: 774–781.

Gloor P, Salanova V, Olivier A, Quesney LF. The human dorsal hippocampal commissure: an anatomically identifiable and functional pathway. *Brain*. 1993:116:1249–1273.

Glover GH, Li T-Q, Ress D. Image-based method for retrospective correction of physiological motion effects in fMRI: RETROICOR. *Magn Reson Med*. 2000:44:162–167.

Gohel SR, Biswal BB. Functional integration between brain regions at rest occurs in multiple-frequency bands. *Brain Connect*. 2015:5: 23–34.

Guo B, Zhou F, Li M, Gore JC, Ding Z. Correlated functional connectivity and glucose metabolism in brain white matter revealed by simultaneous MRI/positron emission tomography. *Magn Reson Med*. 2022::87:1507–1514.

Gupta L, Janssens R, Vlooswijk MCG, Rouhl RPW, de Louw A, Aldenkamp AP, Ulman S, Besseling RMH, Hofman PAM, van Kranen-Mastenbroek VH, et al. Towards prognostic biomarkers from BOLD fluctuations to differentiate a first epileptic seizure from new-onset epilepsy. *Epilepsia*. 2017:58:476–483.

Haneef Z, Lenartowicz A, Yeh HJ, Engel J, Stern JM. Effect of lateralized temporal lobe epilepsy on the default mode network. *Epilepsy Behav*. 2012:25:350–357.

He Y, Chen ZJ, Evans AC. Small-world anatomical networks in the human brain revealed by cortical thickness from MRI. *Cereb Cortex*. 2007:17:2407–2419.

Horovitz SG, Braun AR, Carr WS, Picchioni D, Balkin TJ, Fukunaga M, Duyn JH. Decoupling of the brain's default mode network during deep sleep. *Proc Natl Acad Sci*. 2009:106:11376–11381.

Jia X-Z, Sun J-W, Ji G-J, Liao W, Lv Y-T, Wang J, Wang Z, Zhang H, Liu D-Q, Zang Y-F. Percent amplitude of fluctuation: a simple measure for resting-state fMRI signal at single voxel level. *PLoS One*. 2020:15:e0227021.

Jitsuishi T, Yamaguchi A. Posterior precuneus is highly connected to medial temporal lobe revealed by tractography and white matter dissection. *Neuroscience*. 2021:466:173–185.

Kobayashi E, Grova C, Tyvaert L, Dubeau F, Gotman J. Structures involved at the time of temporal lobe spikes revealed by interindividual group analysis of EEG/fMRI data. *Epilepsia*. 2009:50:2549–2556.

Kowalczyk MA, Omidvarnia A, Dhollander T, Jackson GD. Dynamic analysis of fMRI activation during epileptic spikes can help identify the seizure origin. *Epilepsia*. 2020:61:2558–2571.

Laufs H, Hamandi K, Salek-Haddadi A, Kleinschmidt AK, Duncan JS, Lemieux L. Temporal lobe interictal epileptic discharges affect cerebral activity in "default mode" brain regions. *Hum Brain Mapp*. 2007:28:1023–1032.

Liao W, Zhang Z, Pan Z, Mantini D, Ding J, Duan X, Luo C, Wang Z, Tan Q, Lu G, et al. Default mode network abnormalities in mesial temporal lobe epilepsy: a study combining fMRI and DTI. *Hum Brain Mapp*. 2011:32:883–895.

Mishra A, Li M, Anderson AW, Newton AT, Ding Z, Gore JC. Concomitant modulation of BOLD responses in white matter pathways and cortex. *NeuroImage*. 2020:216:116791.

Morgan VL, Gore JC, Abou-Khalil B. Functional epileptic network in left mesial temporal lobe epilepsy detected using resting fMRI. *Epilepsy Res*. 2010:88:168–178.

Morgan VL, Rogers BP, Abou-Khalil B. Segmentation of the thalamus based on BOLD frequencies affected in temporal lobe epilepsy. *Epilepsia*. 2015:56:1819–1827.

Pereira FR, Alessio A, Sercheli MS, Pedro T, Bilevicius E, Rondina JM, Ozelo HF, Castellano G, Covolan RJ, Damasceno BP, et al. Asymmetrical hippocampal connectivity in mesial temporal lobe epilepsy: evidence from resting state fMRI. *BMC Neurosci*. 2010:11:66.

Pittau F, Grova C, Moeller F, Dubeau F, Gotman J. Patterns of altered functional connectivity in mesial temporal lobe epilepsy. *Epilepsia*. 2012:53:1013–1023.

Salek-Haddadi A, Diehl B, Hamandi K, Merschhemke M, Liston A, Friston K, Duncan JS, Fish DR, Lemieux L. Hemodynamic correlates of epileptiform discharges: an EEG-fMRI study of 63 patients with focal epilepsy. *Brain Res*. 2006:1088:148–166.

Sämann PG, Wehrle R, Hoehn D, Spoormaker VI, Peters H, Tully C, Holsboer F, Czisch M. Development of the brain's default mode network from wakefulness to slow wave sleep. *Cereb Cortex*. 2011:21:2082–2093.

Schilling KG, Blaber J, Huo Y, Newton A, Hansen C, Nath V, Shafer AT, Williams O, Resnick SM, Rogers B, et al. Synthesized b0 for diffusion distortion correction (Synb0-DisCo). *Magn Reson Imaging*. Artificial Intelligence in MRI. 2019:64:62–70.

Smith RE, Tournier J-D, Calamante F, Connelly A. Anatomically-constrained tractography: improved diffusion MRI streamlines tractography through effective use of anatomical information. *NeuroImage*. 2012:62:1924–1938.

Smith RE, Tournier J-D, Calamante F, Connelly A. SIFT2: enabling dense quantitative assessment of brain white matter connectivity using streamlines tractography. *NeuroImage*. 2015:119:338–351.

Tan G, Xiao F, Chen S, Wang H, Chen D, Zhu L, Xu D, Zhou D, Liu L. Frequency-specific alterations in the amplitude and synchronization of resting-state spontaneous low-frequency oscillations in benign childhood epilepsy with centrotemporal spikes. *Epilepsy Res*. 2018:145:178–184.

Tang Y, Yul Choi J, Alexopoulos A, Murakami H, Daifu-Kobayashi M, Zhou Q, Najm I, Jones SE, Irene WZ. Individual localization value of resting-state fMRI in epilepsy presurgical evaluation: a combined study with stereo-EEG. *Clin Neurophysiol*. 2021:132:3197–3206.

Tournier J-D, Calamante F, Connelly A. Robust determination of the fibre orientation distribution in diffusion MRI: non-negativity constrained super-resolved spherical deconvolution. *NeuroImage*. 2007:35:1459–1472.

Tournier J-D, Smith R, Raffelt D, Tabbara R, Dhollander T, Pietsch M, Christiaens D, Jeurissen B, Yeh C-H, Connelly A. MRtrix3: a fast, flexible and open software framework for medical image processing and visualisation. *NeuroImage*. 2019:202:116137.

Wang Z, Zhang Z, Liao W, Xu Q, Zhang J, Lu W, Jiao Q, Chen G, Feng J, Lu G. Frequency-dependent amplitude alterations of resting-state spontaneous fluctuations in idiopathic generalized epilepsy. *Epilepsy Res*. 2014:108:853–860.

Wei W, Zhang Z, Xu Q, Yang F, Sun K, Lu G. More severe extratemporal damages in mesial temporal lobe epilepsy with hippocampal sclerosis than that with other lesions: a multimodality MRI study. *Medicine (Baltimore)*. 2016:95:e3020.

Welch P. The use of fast Fourier transform for the estimation of power spectra: a method based on time averaging over short, modified periodograms. *IEEE Trans Audio Electroacoustics*. 1967:15: 70–73.

Yan C, Liu D, He Y, Zou Q, Zhu C, Zuo X, Long X, Zang Y. Spontaneous brain activity in the default mode network is sensitive to different resting-state conditions with limited cognitive load. *PLoS One*. 2009:4:e5743.

Yan C-G, Cheung B, Kelly C, Colcombe S, Craddock RC, Di Martino A, Li Q, Zuo X-N, Castellanos FX, Milham MP. A comprehensive assessment of regional variation in the impact of head micromovements on functional connectomics. *NeuroImage*. 2013:76: 183–201.

Zang Y-F, He Y, Zhu C-Z, Cao Q-J, Sui M-Q, Liang M, Tian L-X, Jiang T-Z, Wang Y-F. Altered baseline brain activity in children with ADHD revealed by resting-state functional MRI. *Brain Dev*. 2007:29:83–91.

Zhang Z, Lu G, Zhong Y, Tan Q, Chen H, Liao W, Tian L, Li Z, Shi J, Liu Y. fMRI study of mesial temporal lobe epilepsy using amplitude of low-frequency fluctuation analysis. *Hum Brain Mapp*. 2010:31: 1851–1861.

Zhang Z, Xu Q, Liao W, Wang Z, Li Q, Yang F, Zhang Z, Liu Y, Lu G. Pathological uncoupling between amplitude and connectivity of brain fluctuations in epilepsy. *Hum Brain Mapp*. 2015:36: 2756–2766.

Zuo X-N, Di Martino A, Kelly C, Shehzad ZE, Gee DG, Klein DF, Castellanos FX, Biswal BB, Milham MP. The oscillating brain: complex and reliable. *NeuroImage*. 2010:49: 1432–1445.